ANALYSIS OF THE GEOMETRIC ACCURACY OF MSG-SEVIRI IMAGERY FOR ESTIMATION OF CLIMATE VARIABLES

Sultan Kocaman Aksakal, Emmanuel Baltsavias, Konrad Schindler

ETH Zurich, Institute of Geodesy and Photogrammetry
CH-8093 Zurich, Switzerland
sultan.aksakal@geod.baug.ethz.ch, emmanuel.baltsavias@geod.baug.ethz.ch,
konrad.schindler@geod.baug.ethz.ch

*Corresponding author: sultan.aksakal@geod.baug.ethz.ch

ABSTRACT

The geometric accuracy of the images acquired by the SEVIRI instrument aboard the European geostationary satellites MSG-1 and MSG-2 has been investigated in this study. Level 1.5 image data of the High-Resolution Visible (HRV) band with 1-km GSD and several multispectral bands with 3-km GSD at sub-satellite point have been provided by the Swiss GCOS Office at MeteoSwiss. A set of fully automated processing methods has been adopted, developed and implemented for the evaluation of relative and absolute accuracy of the HRV images. For the evaluation of the relative accuracy, large numbers of feature points are extracted and tracked through images of the same day. To assess the absolute accuracy, lakes in the area are used as reference and matched automatically in the HRV images. A number of SEVIRI images acquired in 2008 have been analyzed and relative and absolute shifts of up to about 10 pixels have been observed.

Keywords: MSG-SEVIRI; geometric accuracy; climate variables; remote sensing; computer vision

INTRODUCTION

GCOS (Global Climate Observing System) is a long-term program for monitoring the climate, detect changes, and assess their impacts. It is undertaken by several international organizations including WMO, IOC, UNESCO, UNEP and ICSU (GCOS, 2013). The Swiss GCOS Office at the Federal Office of Meteorology and Climatology (MeteoSwiss) is responsible for coordinating GCOS activities in Switzerland (Seiz et al., 2011).

Remote sensing techniques and satellite imagery are being increasingly used for climate-related measurements and derivation of Essential Climate Variables (ECVs). Satellites are particularly suited for wide-area, repetitive observations of the Earth, even over areas that are difficult to access (Swiss GCOS Office, 2013; WMO, 2011). Under a research agreement between the Swiss GCOS Office at MeteoSwiss and ETH Zurich, the geometric accuracy of image products acquired from three different satellite sensors (SEVIRI aboard the European meteorological satellites of the Meteosat Second Generation Series, MODIS aboard the NASA satellites Terra and Aqua, AVHRR aboard the NOAA and Metop satellite series), which are often used to estimate ECVs, are being investigated. Such investigations are essential, since geometric errors of even modest size modify the location and possibly extent of derived climate variables and conclusions about their change. An example on the impact of band-to-band misregistration errors for MODIS Aqua can be found in Arnold et al. (2010). GCOS has also defined target requirements for geometric accuracy (WMO, 2011).

The project aims include: a) investigation of the relative geometric accuracy within one image, between different channels, and for multi-temporal imagery; b) investigation of the absolute geometric accuracy using reference data; c) investigation of the temporal stability of the absolute as well as the relative geometric accuracy; d) preliminary analysis of the impact of geometric errors on the derivation of climate variables. In particular, we investigate whether the geometric accuracy specifications of the related sensor products are really fulfilled over Switzerland.

In the first stage of the project, the relative and absolute geometric accuracies of the HRV (High-Resolution Visible) channel of SEVIRI (Spinning Enhanced Visible and Infra-Red Imager) have been investigated. The SEVIRI instrument is designed to support nowcasting, numerical weather forecasting, and climate applications over Europe and Africa (Aminou et al., 2003). It combines the East-West scan generated by the satellite spin motion and the South to North micro-step scan of a

mirror. The instrument generates images of the Earth in 12 different spectral channels, from visible to infrared, with 1 km and 3 km Ground Sample Distances (GSDs) (Eumetsat, 2010). For the HRV channel, there are 9 detectors, and 9 lines are obtained per satellite revolution at 1 km GSD (nominal at Sub Satellite Point - SSP) with spectral bandwidth of 0.6-0.9 µm.

The SEVIRI instruments acquire images aboard Meteosat-8 (formerly MSG-1) and Meteosat-9 (formerly MSG-2). During the period which was selected for investigations in this project, SEVIRI aboard Meteosat-9 was in operation as the main instrument and Meteosat-8 was used as stand-by. In case of unavailability of Meteosat-9, a satellite swap was performed and Meteosat-8 was operated as the primary mission.

EUMETSAT corrects the raw image (Level 1.0) in real-time for all radiometric and geometric effects, and georeferences it using a standardized projection (Eumetsat, 2010). The resulting Level 1.5 image consists of georeferenced, calibrated and radiance-linearized information for the derivation of meteorological products and other meteorological processing (Eumetsat, 2010; Just, 2000). The absolute accuracy specification for SEVIRI Level 1.5 data from Meteosat-8 and Meteosat-9 is < 3.0 km (EUMETSAT, 2007). The relative accuracy specifications between two consecutive images and within an image (over 500 samples) are < 1.2 km and < 3.0 km, respectively.

There have been a few studies in the literature reporting the geometric accuracy of the SEVIRI imagery. Hanson et al. (2003) conducted some tests on the absolute and relative geometric accuracies of the SEVIRI aboard Meteosat-8 during the commissioning phase. They have reported that the geometric performance meets the specifications, usually with a significant margin. Hanson and Müller (2004) have reported up to 3 pixels image shift in East-West direction immediately after eclipse for the multispectral (MS) channels of Meteosat-8. Gieske et. al. (2005) have reported that the geocoding accuracy for Meteosat-8 is typically in the order of 1 pixel for the MS imagery. However, in the analysis of image time series it was also noted that sometimes shifts are observed. Dürr and Zelenka (2009) have used HRV and MS images that are acquired between 2004-2006 from Meteosat-8 and Meteosat-9 in their study and improved the geolocation of the HRV imagery. They have applied a similar approach as proposed here and used lakes in order to compute shifts at pixel level accuracy on the HRV images over Alpine areas. They have observed shifts up to 8 pixels to the North. Aksakal (2013) has reported the methodology and the initial test results with the HRV data for this study.

METHODOLOGY

In order to achieve the project goals, a set of fully automated processing methods has been adopted, developed and implemented; using tools from photogrammetry, image processing and computer vision. A stand-alone software package is being implemented in Python 2.6 programming language for highly automated processing of the SEVIRI data (Aksakal, 2013). For relative accuracy assessment, a large number of feature points (≈300-1000) are extracted and tracked through the images of the same day, using the KLT (Kanade-Lucas-Tomasi) tracker (Lucas and Kanade, 1981) extended with statistical analysis and blunder detection procedures to ensure a robust evaluation without matching errors. To assess absolute accuracy, lakes (with a sufficient size) in the area are used as reference and the lake boundaries are matched in the images via 2D sub-pixel translations.

Relative Accuracy Evaluation

The relative accuracy is evaluated for sequences of consecutive HRV images acquired on the same day, in order to have very small illumination differences between the images used for matching. For each day selected for processing, 17 images acquired between 9:00-13:00 UTC are used for the evaluation of 2D translation errors. The processing steps for the relative accuracy investigations with the HRV channel data are depicted in Figure 1.

The feature points are extracted from the selected first image of the day (9 o'clock) and matched in the consecutive image (i.e. taken at 9:15). The given HRV cloud masks are integrated in the feature point selection process in order to exclude cloud regions. After matching, statistical values are calculated for the whole point set based on the image coordinate differences with signs ($\Delta x,\Delta y$) for both axes (x,y): *Mean, standard deviation* (σ), *median* (*MED*), *median absolute deviation* (*MAD*) from the median, *minimum*, and *maximum* values. Every ($\Delta x,\Delta y$) is compared against the *mean-x* and *mean-y*, respectively; and the ones having an absolute difference larger than 3σ are considered as outliers.

The *MED* and *MAD* values are used for a final comparison with the *mean* and σ values, in order to analyze existence of any remaining outliers in the dataset ($\sigma \cong 1.48*MAD$). The blunders usually occur in low contrast and low texture areas and are caused by matching errors. The outlier check is repeated iteratively until a blunder-free set is obtained. The ($\Delta x, \Delta y$) are plotted on a preprocessed reference image for an optional visual assessment of the errors, in terms of location, direction and magnitude.

The matching process continues until the last image of the day, which is selected as 13:00 image for this evaluation. The successfully matched points are used as candidate points for the next pair of images (e.g. 9:15 and 9:30). If the total number of points after the blunder detection falls below a given threshold, new points are added to the candidate list based on the earlier image of the new pair and the cloud mask. In practice, the total number of points is usually above 500 and the percentages of matching outliers are in the range of 3%-20%, with an average of 10%. The spatial distribution of the points in non-cloudy areas is adequate for relative accuracy evaluation purposes.

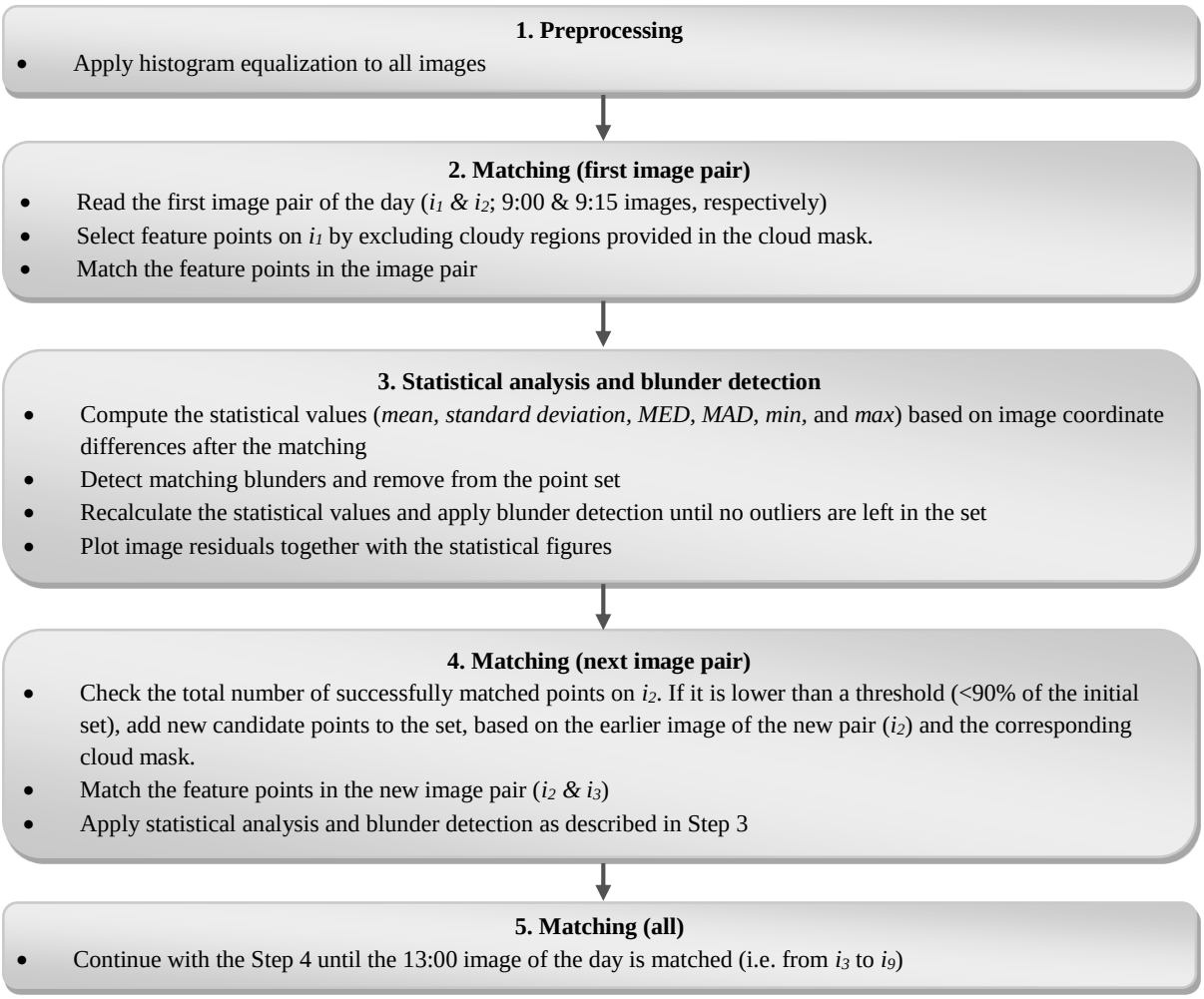

Figure 1. The processing chain for the relative accuracy evaluation of SEVIRI HRV image sequences.

Absolute Accuracy Evaluation

Absolute accuracy evaluation of the MSG-SEVIRI imagery is done based on lakes, since the detection of shorelines in the HRV images is relatively easy and reliable and lakes are the only detectable objects with a good contrast to the land. The approach in this study is based on the observation that the pixel grey values of the lakes in the HRV images are low (typically less than 30), and the water pixels are always darker than the surrounding lake-shores.

A total of 40 lakes are manually digitized into vector polygons from two different Landsat orthophotos (Aksakal, 2013) and used as reference. The polygons are transformed into the HRV image space. After visual inspection and initial tests for matching, small lakes, which cover an area of

smaller than 7 pixels, are removed from the evaluation. The remaining 20 lakes are used for the investigations.

For the matching, each lake polygon is moved inside a 20x20 pixels search window (i.e. ± 10 pixels) starting from its initial position. This window size has been found sufficient for the tests. A coarse-to-fine matching is performed in two steps: first, 1 pixel step size is applied to have an approximate matching; and second, the results obtained from the first matching are refined within a range of 1.2x1.2 pixels (i.e. ± 0.6 pixels). For the fine matching, a step size of 0.1 pixel is selected in order to achieve sub-pixel accuracy. At each step, the normalized sum of pixel intensities inside the lake polygons is computed (Aksakal, 2013). The partial pixels at the polygon edges are also added to the sum with respect to the pixel area that falls inside the polygon.

The minimum of the normalized sums is selected for each lake within a given image. The step parameters ($\Delta x,\Delta y$), which provide the minimum sum are considered the shift of the lake. The algorithm for matching a lake polygon in the HRV image is depicted in Figure 2. The statistical values (*mean*,σ, *MED*, *MAD*, *min*, *max*) are derived from the shifts of all lakes in an image. After initial experiments, lakes having a cloud cover >40% are excluded from the process, since the matching is usually not successful.

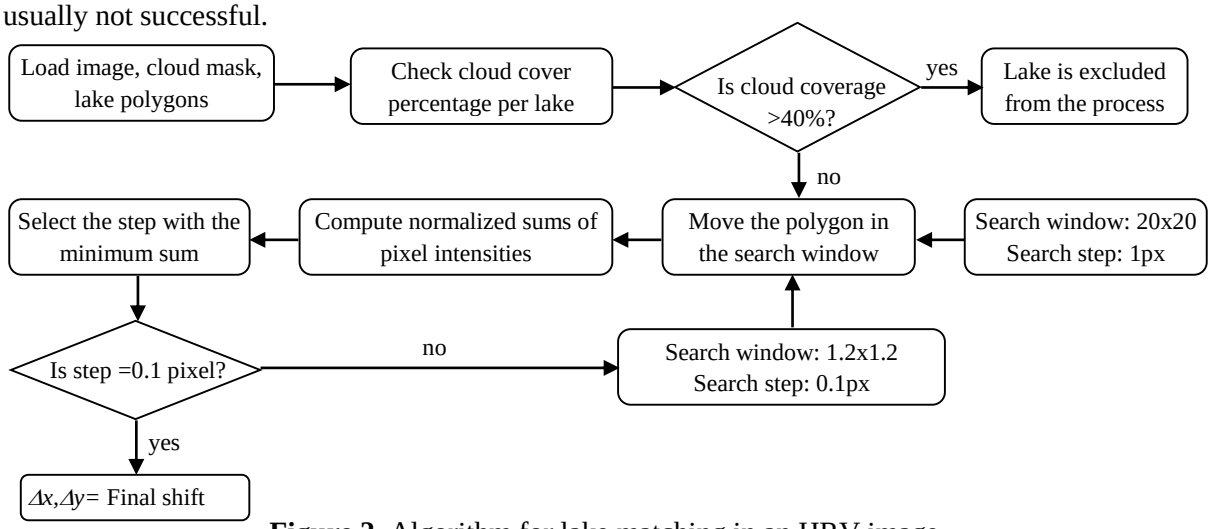

Figure 2. Algorithm for lake matching in an HRV image.

RESULTS AND DISCUSSION

Since the main aim is to analyze data quality over Switzerland, HRV image parts covering a rectangular area over Switzerland and surrounding countries from 2008 have been used with a size of 652 x 393 pixels. The GSD of the image pixels in the project area varies in the range of 1-2 km. The HRV image part acquired on 30.08.2008 at 12:00 UTC and all lakes used for absolute accuracy evaluation can be seen in Figure 3. A cloud mask with the same spatial resolution is integrated in the processing of each HRV image. Although the images have been acquired mainly from Meteosat-9, there is a substantial amount of imagery from Meteosat-8 throughout the year. In addition, gaps have occurred in the image sequences on several days.

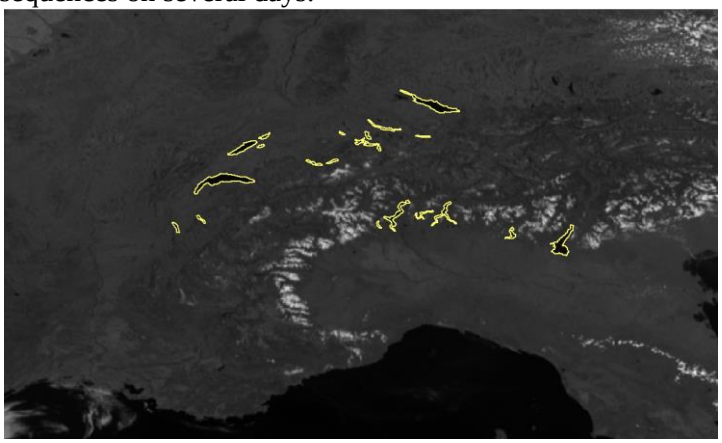

Figure 3. HRV image part from 30.08.2008 and the lakes used for absolute accuracy investigations.

The absolute accuracy investigations and the first relative accuracy investigations have been performed using the HRV images from 24 different days (two days from each month with minimum cloud coverage) in 2008 (Aksakal, 2013). In the analysis, relative shifts up to 8 pixels have been observed between consecutive images on several days, on which the data have been acquired with Meteosat 8. Therefore, relative accuracy investigations have been performed using the images acquired on 103 additional days. The remaining days are not processed due to high cloud coverage.

Relative Accuracy Investigations

The relative accuracy investigation methods developed here are tested using a total of 2111 HRV images acquired on 127 different days, between 9:00-13:00 UTC. There have been processing gaps on some days due to high cloud coverage or data unavailability. The results are provided for Meteosat-8 and Meteosat-9 in Table 1. In addition, the HRV data of 4 different days, where the image sequences contain data from both satellites, have been analyzed separately and the results are provided in the lower part of the Table. The number of points matched in consecutive image pairs for all 127 days is in the range of 211-1037, with an average of 570.

Table 1. Statistical summary of the relative shifts from all image pairs for all 127 days (in pixels).

Satellite	Value	Mean (x)	Mean (y)	MED (x)	MED (y)	σ (x)	σ (y)	MAD (x)	MAD (y)
Meteosat-8	Min	-1.20	-9.59	-1.20	-9.59	0.03	0.02	0.02	0.01
	Max	1.13	9.42	1.14	9.44	0.28	0.30	0.17	0.16
	Mean	-0.04	0.06	-0.04	0.06	0.07	0.08	0.04	0.05
Meteosat-9	Min	-0.30	-1.39	-0.30	-1.39	0.03	0.02	0.02	0.02
	Max	0.31	0.77	0.33	0.77	0.30	0.30	0.17	0.18
	Mean	-0.02	-0.01	-0.02	-0.01	0.11	0.12	0.06	0.08
Meteosat-8& Meteosat-9	Min	-0.99	-0.39	-1.00	-0.42	0.03	0.04	0.02	0.03
	Max	0.86	1.42	0.87	1.39	0.21	0.23	0.14	0.16
	Mean	-0.06	0.01	-0.07	0.01	0.06	0.09	0.04	0.06

The results of Meteosat-8 are obtained from the images of 24 different days (16 days in February, 5 days in March, single days in May, November, and December 2008). The *Min* and *Max* values for the $Mean_x$ and $Mean_y$ of Meteosat-8 data show that the relative shifts occur in all directions. However, the variations are larger along the y axis (up to 9.6 pixels). The minus sign shows shifts to West and South for *x* and *y*, respectively. The *Mean* and *MED* values of the shifts are quite similar, showing that no big blunders exist in the results. The mean σ_x and σ_y are slightly less than 0.1 pixels, which can be considered as matching accuracy. The higher standard deviations (up to 0.30 pixels) occurred on the days where the images were largely covered with clouds, and thus the matching was more difficult.

In the results of Meteosat-9 in Table 1, shifts up to 0.30 and 1.39 pixels for *x* and *y* are observed in the *Min* and *Max* values for the $Mean_x$ and $Mean_y$. The *MED* values are also similar to the *mean* values. The *mean* σ values obtained from the matching of all 1542 pairs are again around 0.1 pixels, as in the Meteosat-8 results. In comparison to Meteosat-8, the relative accuracy of Meteosat-9 is higher, i.e. the geolocalization is more stable.

The statistical parameters computed from the images acquired on 4 different days (19.11, 26.11, 27.11. and 07.12.2008) can also be found in Table 1. On these days, multiple satellite swaps occurred and the sequences contain images from both satellites. The larger shifts have been observed during the swaps, where the image pair is composed of one Meteosat-8 and one Meteosat-9 image.

A graphical representation of relative shifts obtained over 127 days is given in Figure 4. The main observation is that large shifts are present between 01.02.2008-19.02.2008, and only when Meteosat-8 was in operation as primary mission. On later days, also Meteosat-8 delivers stable images.

A detailed analysis has been done for one image pair (10:30-10:45) acquired from Meteosat-8 on the 7th of February. After the matching, the image space residuals are plotted on a preprocessed image for visual assessment of the results. The $Mean_x$ and $Mean_y$ values of the residuals are 0.8 and -7.0 pixels, respectively. Both the σ_x and σ_y are 0.1 pixels. Two residual plots, before and after the removal of the mean shift, are shown in Figure 5. The remaining residuals do not show any systematic effect, which implies existence of only 2D shift errors between the images. The even distribution of the residuals also implies high relative accuracy within the image.

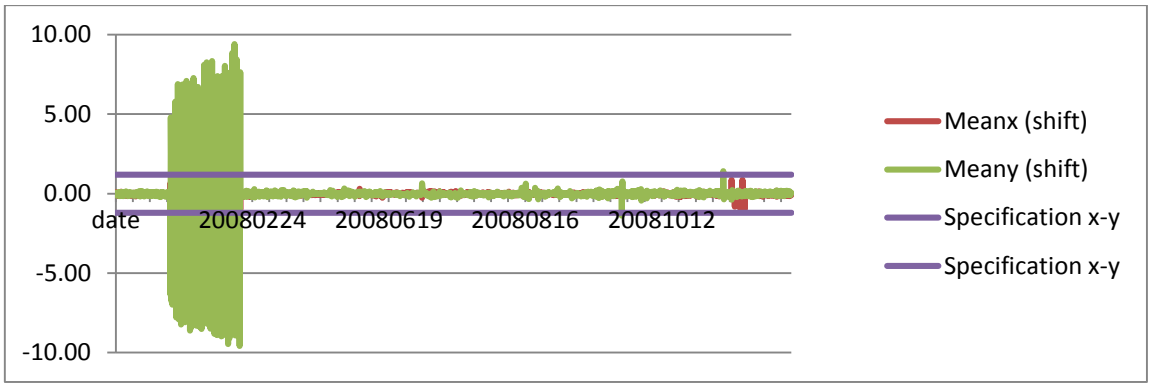

Figure 4. Relative shifts (in pixels) obtained from the images acquired on 127 days between 9:00-13:00 in 2008. The horizontal axis denotes the date.

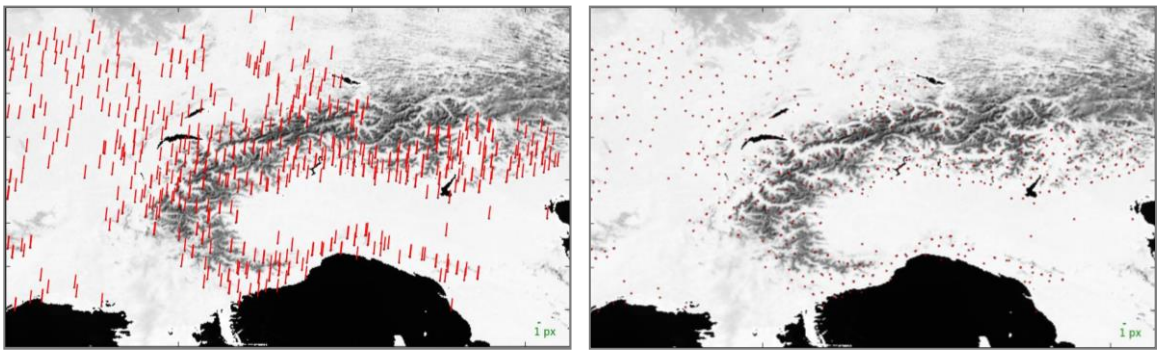

Figure 5. 2D image space residuals before (left) and after (right) removal of the mean 2D shifts between the 10:30 and 10:45 images acquired on the 07.02.2008.

Absolute Accuracy Investigations

The lake matching is applied to the HRV images acquired on 24 different days (two days from each month) at 12:00 and the results are summarized in Table 2. Positive values indicate shifts to the North and East, respectively. The range for the number of lakes used for the Meteosat-9 evaluations is 6-20, with a mean of 16, the variations being caused by clouds. For Meteosat-8, the number of lakes ranges from 12-19, with a mean value of 17. Figure 6 shows zoomed images with different lakes. The yellow and the green lake polygons denote the initial and the final positions before and after the matching. It can be seen in Figures 6b and 6c that lakes partially covered by clouds can also be used for the evaluations.

The statistical values given in Table 2 for Meteosat-8 are derived from the estimated shift values of individual lakes for 5 days. The *Min, Max, Mean* and *MED* values are computed from the statistical values of all 5 images. All images are shifted to North and East. The variation in y is larger, between 0.3 to 3.3 pixels, showing poorer stability of the sensor in this direction. The σ values calculated from the individual lake offsets are in the range of 0.1-0.3 pixels, with a mean standard deviation of 0.2 pixels, which shows the mean accuracy of the matching. This value can also be interpreted as the variability of absolute accuracy among the lakes of one image.

The statistical values in Table 2 for Meteosat-9 are derived from the estimated shift values of individual lakes for 19 days. The *Min, Max, Mean* and *MED* values are derived from the results of all 19 images. All images are shifted to North and East, with a max shift of 1.4 pixels for x and 3.0 pixels for y. Similar to the Meteosat-8 results, the mean σ values calculated from the individual lake offsets are in the range of 0.1-0.3 pixels, with a mean σ of 0.2 pixels. When the results of both satellite datasets are compared, no significant accuracy differences have been observed between the two satellites. However, it should be noted that the results given in Table 2 have been obtained from the 12:00 images only. The large relative shifts (up to 10 pixels, see previous section) imply also large absolute accuracy errors. Figure 7 shows the results of an in depth analysis for two days, where the images were acquired with Meteosat-8 (8th of February) and Meteosat-9 (30th of August). The

analysis has shown that some of the Meteosat-8 images have also large absolute accuracy errors (up to 8 pixels).

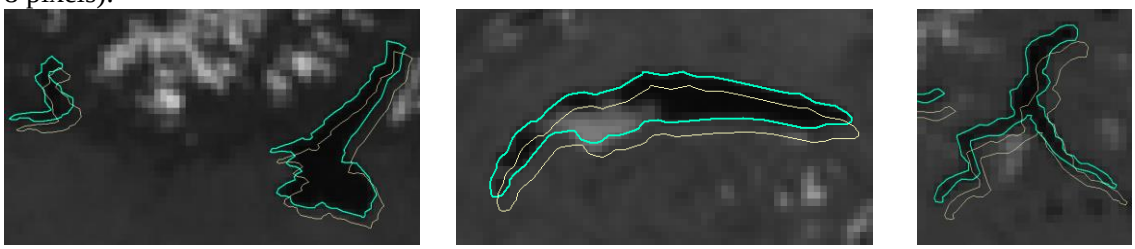

Figure 6. a) Iseo and Garda Lakes (left); **b)** Leman Lake (middle); and **c)** Como Lake (right). The yellow and green polygons denote the initial positions and the matched positions.

Table 2. Absolute accuracy evaluation; statistical summary from the shifts of 12:00 images.

Satellite		Mean (x)	Mean (y)	Mean (xy)	σ (x)	σ (y)	MED (x)	MED (y)	MAD (x)	MAD (y)
Meteosat-8	Min	0.5	0.3	0.9	0.1	0.2	0.5	0.3	0.1	0.1
	Max	1.5	3.3	3.3	0.2	0.3	1.4	3.3	0.2	0.2
	Mean	1.0	1.9	2.3	0.2	0.2	1.0	1.9	0.1	0.2
	MED	0.9	2.0	2.4	0.2	0.2	0.9	2.0	0.1	0.2
Meteosat-9	Min	0.3	1.8	2.1	0.1	0.1	0.4	1.7	0.0	0.1
	Max	1.4	3.0	3.1	0.3	0.3	1.3	3.0	0.1	0.2
	Mean	0.9	2.3	2.5	0.2	0.2	0.9	2.3	0.1	0.1
	MED	1.0	2.2	2.4	0.2	0.2	1.0	2.2	0.1	0.1

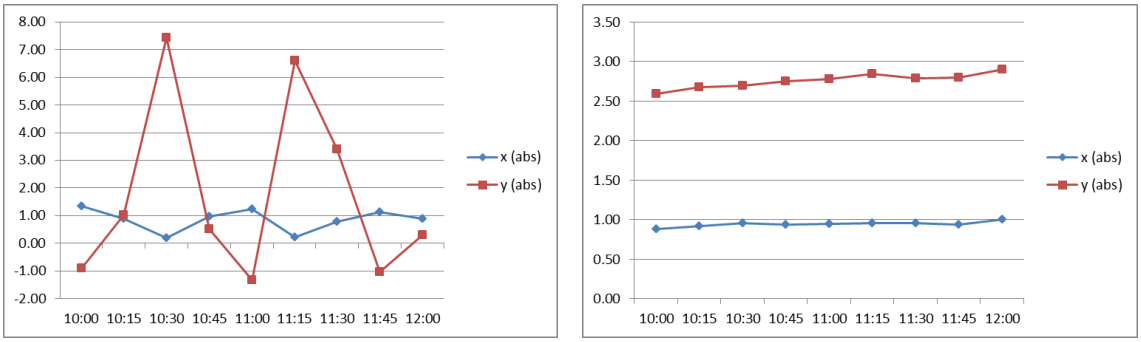

Figure 7. Absolute shifts for the images acquired on the a) 08.02.2008 with Meteosat-8 (left); b) 30.08.2008 with Meteosat-9 (right). Horizontal axis: image acquisition time; Vertical axis: pixel.

CONCLUSIONS AND FUTURE WORK

Under a research contract with the Swiss GCOS Office, the geometric accuracy of a number of meteorological satellites is being investigated. In this study, a set of algorithms for the relative and absolute geometric accuracy evaluation of the SEVIRI aboard the European geostationary satellites Meteosat-8 (MSG-1) and Meteosat-9 (MSG-2) data has been developed and tested. The geometrically preprocessed HRV Level 1.5 imagery is used for algorithm development and the evaluations. The proposed methods provide a robust and fully-automatic accuracy assessment for the HRV imagery with sub-pixel accuracy.

Only HRV data over Switzerland are evaluated. The results show that there are large relative shifts (up to 10 pixels) between consecutive images (15 minutes interval). Further analysis also shows that the large shifts occurred only with Meteosat-8 during 1-19 February, 2008. The SEVIRI on Meteosat-9 delivers more stable images and the maximum relative shift is 1.4 pixels. The absolute accuracy values computed from the 12:00 images of 24 days show that shifts up to 1.5 pixels to the East and up to 3.3 pixels to the North are present. However, further analysis on the Meteosat-8 images acquired at earlier hours with large relative shifts has shown that these images have also large absolute geolocation errors. The mean values obtained from the absolute shifts of 19 Meteosat-9 images are 0.9 (in *x*) and 2.3 (in *y*) pixels.

The values obtained from the Meteosat-8 images are higher than the accuracy specifications by EUMETSAT, which are 1.2 km (1.2 pixels for HRV) relative between consecutive images, and 3 km (3 pixels for HRV) absolute. The inferior geometric accuracy and the occasional instability of the

sensor should be taken into consideration for climate-related measurements and other applications of SEVIRI.

Algorithms and tools to assess the band-to-band registration accuracy are currently being developed and tested. Similar investigations will be performed with the data of two other satellite sensors, namely MODIS and AVHRR.

ACKNOWLEDGMENTS

This study is supported by the Swiss GCOS Office at the Federal Office of Meteorology and Climatology (MeteoSwiss). The authors thank the members of the Swiss GCOS Office for providing data and their valuable inputs.

REFERENCES

Aksakal, S.K., 2013, Geometric Accuracy Investigations of SEVIRI High Resolution Visible (HRV) Level 1.5 Imagery, *Remote Sensing*, (5), 1-x manuscripts; doi:10.3390/rs50x000x.

Aminou D.M.A., Luhmann H. J., Hanson C., Pili P., Jacquet B., Bianchi S., Coste P., Pasternak F., Faure F., 2003, Meteosat Second Generation: A comparison of on-ground and on-flight imaging and radiometric performances of SEVIRI on MSG-1, *Proceedings of the 2003 EUMETSAT Meteorological Satellite Conference*, Weimar, Germany, 29 September-3 October, 236-243.

Arnold, G.T; Hubanks, P.A.; Platnick, S.; King, M.D.; Bennartz, R., 2010, Impact of Aqua Misregistration on MYD06 Cloud Retrieval Properties. Presented at *MODIS Science Team Meeting*, Washington, DC, USA, 26–28 January. Available online: http://modis.gsfc.nasa.gov/sci_team/meetings/201001/presentations/posters/atmos/arnold.pdf (accessed on 11 Sep. 2013).

Dürr B., Zelenka A.,2009, Deriving surface global irradiance over the Alpine region from Meteosat Second Generation by supplementing the HELIOSAT method, *International Journal of Remote Sensing*, 30(22), 5821–5841, doi: 10.1080/01431160902744829.

EUMETSAT, 2007, Typical Geometrical Accuracy for MSG-1/2, Doc. No: EUM/OPS/TEN/07/0313 v1, 26 February 2007.

EUMETSAT, 2010, MSG Level 1.5 Image Data Format Description, Document no: EUM/MSG/ICD/105, Issue v6, 23 February 2010.

GCOS, 2013, http://www.wmo.int/pages/prog/gcos/ (last accessed on 12.08.2013).

Gieske A.S.M., Hendrikse J.H.M., Retsios V., van Leeuwen B., Maathuis B.H.P., Romaguera M., Sobrino J.A., Timmermans W.J., Su Z., 2005, Processing of MSG - 1 SEVIRI data in the thermal infrared - algorithm development with the use of the SPARC2004 data set, *Proceedings of the ESA WPP-250 SPARC Final Workshop*, 4-5 July.

Hanson C., Mueller J.,2004, Status of the SEVIRI Level 1.5 Data, *Proceedings of the Second MSG RAO Workshop* (ESA SP-582, November 2004), Salzburg, Austria, 9 - 10 September, available at: http://earth.esa.int/workshops/msg_rao_2004/papers/4_hanson.pdf (last accessed on 12.08.2013).

Hanson C.G., Mueller J., Pili P., Aminou D.M.A., Jacquet B., Bianchi S., Coste P., Faure F., 2003, Meteosat Second Generation: SEVIRI Imaging Performance Results From The MSG-1 Commissioning Phase, *The 2003 EUMETSAT Meteorological Satellite Conference*, Weimar, Germany, 29 September-3 October.

Just D., 2000, SEVIRI Level 1.5 Data, *Proceedings of the First MSG RAO Workshop* (ESA SP-452, October 2000), Bologna, Italy, 17-19 May.

Lucas, B.; Kanade, T.,1981, An Iterative Image Registration Technique with an Application to Stereo Vision. *Proceedings of 7th International Joint Conference on Artificial Intelligence (IJCAI)*, Vancouver, BC, Canada, 24–28 August.

Seiz G., Foppa N., Meier M., Paul F., 2011, The role of satellite data within GCOS Switzerland, *Remote Sensing*, (3), 767-780, doi: 10.3390/rs3040767.

Swiss GCOS Office, 2013, GCOS Satellite Component, http://www.meteoschweiz.admin.ch/web/en/meteoswiss/international_affairs/gcos/Satellites.html (last accessed on 12.08.2013).

WMO, 2011, Systematic Observation Requirements for Satellite-based Products for Climate, Supplemental details to the satellite-based component of the Implementation Plan for the Global Observing System for Climate in Support of the UNFCCC (Update). GCOS-154.